Nonlinear Dynamics In Mode Locked Lasers: Modeling, Simulations And Analysis

Radziunas M.
Weierstrass Institute for Applied Analysis and Stochastics
Leibniz Institute in Forschungsverbund Berlin e. V.
Mohrenstr. 39, 10117, Berin, Germany

***Abstract* – In this work, we present two distinct approaches for modeling of mode-locked lasers. These models are based on the first order partial differential equations for counter-propagating optical fields and the delay differential equation for a one-directionally propagating field, respectively. We demonstrate how simulations and different type of analysis of these models allow us to get a better understanding of various peculiarities of the complicated dynamics in ML lasers and helps to improve the design of the devices.**

***Key words* – mode-locked laser, pulsations, semiconductor, traveling wave model, delay differential equation model, simulations, analysis.**

I. Introduction

Mode-locked (ML) edge-emitting semiconductor lasers are widely used for generation of short optical pulses with repetition rates of a few to hundred GHz. Modeling, simulation and analysis of mode locking in single- or multi-section quantum-well, quantum-dash or quantum-dot semiconductor lasers plays a crucial role seeking to understand and control various instabilities of the ML lasers.

Mode-locking can be observed in semiconductor laser devices of different geometry. For example, it was found in edge-emitting lasers with an external modulator; vertical-cavity, edge-emitting or ring lasers with a single or several integrated or external saturable absorbers (SAs) [1-5], see Fig. 1(a); or single-section quantum-dash or quantum-dot based Fabry-Perot (FP) type edge-emitting lasers [6].

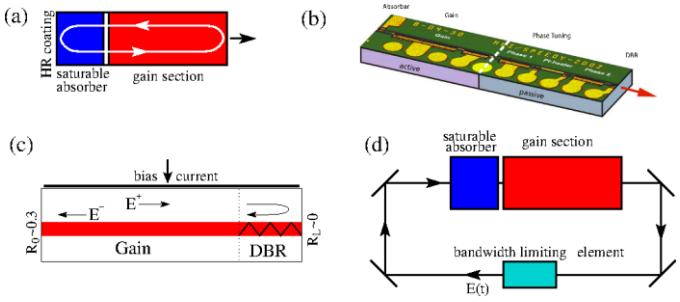

Fig. 1. Schematic representation of several ML lasers.

ML lasers can also have several amplifying, passive or distributed Bragg reflector (DBR) sections supplemented by individual electrical contacts, see Refs. [1,2,6] and Fig. 1(b) and (c)]. These additional sections provide a better control of the laser operating states. For example, DBR sections allow a better control of the emission wavelength [2] or a better integration of the ML laser into the optical circuits [6]. To improve the quality of already emitted ML pulsations, one can also apply an additional forcing. It can be a periodic modulation of the SA voltage [5], an injection of a single or several coherent external optical beams, or a reinjection of the emitted field with an appropriately selected time delay.

Mode-locking itself is an operation regime of the laser during which a periodic sequence of short optical pulses is emitted, and the period of this sequence is strictly determined by the field roundtrip time in the laser cavity. Short optical pulses, in this case, are due to a superposition of multiple, in the frequency domain equally separated longitudinal optical modes, having a certain fixed (locked) phase relation between each other. A simple example of the ML pulsations is given by a complex (field emission) function $E(t)=\sum_{j=1}^{n} f_j(t)$. Here, $f_j(t)=\bar{f}e^{i\chi_j}e^{i(\varphi+\Delta j)t}$ is the contribution of j-th optical mode, $\varphi+\Delta j$ is the mode frequency, and the relative phases χ_j of all modes are locked by a single linear relation $\chi_j=-(\varphi+\Delta j)\tau$. Then the field intensity $|E(t)|^2=\bar{f}^2\sin^2\left(\frac{\Delta n(t-\tau)}{2}\right)\Big/\sin^2\left(\frac{\Delta(t-\tau)}{2}\right)$ has short pulses at $t=\tau \mod(2\pi/\Delta)$.

Several more realistic simulated periodic states of some ML laser are presented in Fig. 2. The top row diagrams represent a fundamental ML state having a single short-pulse emission during the field roundtrip time T in the laser cavity. For different gain section bias current or negative SA voltage, one can also find other periodic states, such as harmonic ML pulsations (two equal pulses during the time T and high suppression of each second spectral line in radio-frequency (RF) and optical spectra, see second row of Fig. 2), pulses with broad trailing edges (third row of Fig. 2) or emission of two or more different pulses during the same time T (fourth row of Fig. 2). Moreover, besides of the regular periodic states one can also observe a variety of irregular "imperfect" mode-locking states having significant time jitter and small side mode suppression in the RF spectrum.

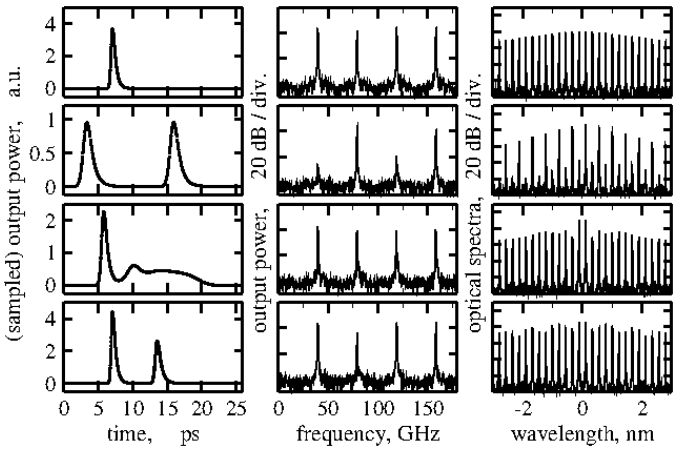

Fig. 2. Four typical simulated periodic states of the ML laser. Left: field emission during a single field roundtrip in the cavity. Middle: radio-frequency spectra. Right: optical spectra.

Below in this work we present two distinct approaches for modeling of mode-locked lasers. The first approach is based on the traveling wave (TW) model, which is a system of one-dimensional first-order PDEs resolving temporal-longitudinal dynamics of the counter-propagating optical fields and carriers [7]. Another method is given by a system of delay differential equations (DDEs) for a one-directional propagation of optical fields in the ring cavity (Fig: 1(d)) and carriers [8]. Both these models are widely used not only for numerical simulation of different ML lasers, but also for a detailed analysis of the typical operating regimes of ML lasers. In this work, we briefly present several analytic and semi-analytic methods for analysis of model equations. We show, how these methods give a better understanding of the complicated dynamics in ML lasers, allow to improve existing or predict new operation regimes, as well as to improve the design of the ML devices.

II. Optical modes of the TW model

The traveling wave equations [7] of multi-section edge-emitting semiconductor laser can be written in the following operator form:

$$-i\partial_t\Psi(z,t)=H(\beta)\Psi(z,t),\ \Psi=\left(E^+,E^-,p^+,p^-\right)^T,$$
$$H\left(\beta(z,t)\right)=\begin{bmatrix}H_0(\beta)+\frac{iv_g\bar{g}}{2}I & -\frac{iv_g\bar{g}}{2}I\\ -i\bar{\gamma}I & (\bar{\omega}+i\bar{\gamma})I\end{bmatrix},$$
$$H_0(\beta)=v_g\begin{bmatrix}i\partial_z-\beta & -\kappa^-\\ -\kappa^+ & -i\partial_z-\beta\end{bmatrix},\quad I=\begin{bmatrix}1&0\\0&1\end{bmatrix},\qquad (1)$$
$$E^+(0,t)=\sqrt{R_0}E^-(0,t),\quad E^-(L,t)=\sqrt{R_L}E^+(L,t).$$

Here, the four-component vector-function $\Psi(z,t)$ represents the slowly varying complex amplitudes of the counter-propagating optical fields, $E^{\pm}$, and polarization functions, $p^{\pm}$, which together with the parameters $\bar{\omega}$, $\bar{\gamma}$, and $\bar{g}$ are used to model the material gain dispersion. v_g is the group velocity, $\kappa^{\pm}$ is the field coupling factor within the DBR sections, R_0 and R_L are the field intensity reflections at the laser facets z=0 and z=L. Function β is the wave propagation factor depending on the dynamically changing carrier density within the active and SA parts of the device. For the considered dynamical models of carriers in quantum-well and quantum-dot based lasers see Refs. [7] and [3], respectively.

Usually, the dynamics of carriers is slow so that in any short time interval β remains nearly constant. For each fixed distribution $\beta(z)$ the operator $H(\beta)$ from Eq. (1) together with the boundary conditions for the fields $E^{\pm}$ gives rise to the spectral problem [9]

$$\Omega(\beta)\theta(\beta,z)=H(\beta)\theta(\beta,z),\quad \theta=\left(\theta_{E^+},\theta_{E^-},\theta_{p^+},\theta_{p^-}\right)^T,$$
$$\theta_{E^+}(\beta,0)=\sqrt{R_0}\theta_{E^-}(\beta,0),\quad \theta_{E^-}(\beta,L)=\sqrt{R_L}\theta_{E^+}(\beta,L). \qquad (2)$$

All complex-valued sets $\left(\theta(\beta,z),\Omega(\beta)\right)$ satisfying Eq. (2) are instantaneous longitudinal optical modes of the considered system. After the suitable normalization of the eigenfunctions $\theta(\beta,z)$ (by, e.g., assuming $\theta_{E^-,j}(\beta,0)=1$), the field function $\Psi(z,t)$ can be represented as sum of suitably normalized modal components:

$$\Psi(z,t)=\sum\nolimits_j f_j(t)\theta_j(\beta,z),\quad f_j(t)\propto\exp\left(i\bar{\Omega}_j t\right). \qquad (3)$$

Here, $\bar{\Omega}_j$ are time averages of the complex eigenvalues, $\Omega_j\left(\beta(z,t)\right)$, $\mathrm{Im}\,\Omega_j$ determines growth/decay of the mode, and the optical frequencies $\mathrm{Re}\left(\bar{\Omega}_j\right)$ are nearly equidistant for the FP-type lasers.

We have used a mode expansion (3) of the optical field and its consequent reconstruction from only several selected modes for investigation of the broad ML pulses observed experimentally in standard two-section quantum-dot lasers [3,4].

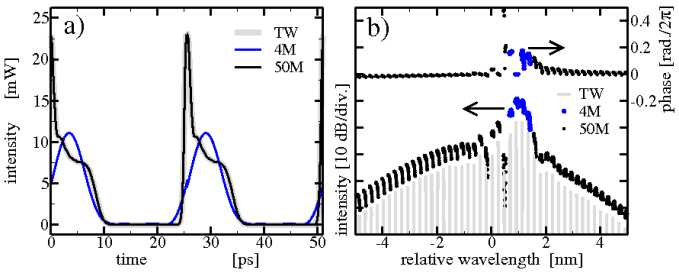

Fig. 3. Simulated ML pulsations with a broad trailing edge plateau [4]. (a): Calculated time trace of the field intensity [thick gray curve] and its reconstruction using 4 and 50 modes with largest amplitudes [thin curves]. (b): optical spectra [grey lines], the relative mode phases (above) and mode amplitudes (below) vs. relative mode wavelengths [bullets].

Our theoretical study presented in Fig. 3 has shown that the shape of the simulated ML pulse depends strongly on the relations between the amplitudes and phases of the complex

modal functions $f_j(t)$. The complex emitted field function in the considered case can be represented as a sum of two functions, both determined by the superposition of several modes. The first of these functions is the sum of all modes with almost zero relative phases (black upper bullets in Fig. 3(b)) and similar intensities, decaying uniformly with an increasing mode frequency (wavelength) separation from the gain peak frequency (black lower bullets in the same figure). This function is responsible for the main sharp field intensity peak of the ML regime (see Fig. 3(a)). The second function is determined only by a few most intensive modes (after subtracting their moderate contribution to the first function) with the relative phases located along some slanted line (upper blue bullets in Fig. 3(b)). The 4-mode reconstruction of the optical field (blue curve in Fig. 3(a)) has a related ~20% of period peak intensity dislocation. The superposition of two such complex periodic functions with different peak intensity positions implies a strong asymmetry of the ML pulse.

Another application of our mode analysis was given in Ref. [8]. In this case, we have analyzed ML pulsations in quantum dash based lasers consisting of a single active section and three different monolithically integrated DBR sections at the right side of the device. In all cases, the length of the whole device was kept constant, whereas the length l_{DBR} and the coupling κ_{DBR} of the DBR part were (250 μm, 40/cm), (50 μm, 200/cm), and (25 μm, 400/cm), respectively. Measurements of these devices have shown, that the quality of ML pulsations in the laser with κ_{DBR}=400/cm was comparable to that one of the simple FP type laser. On the other hand, the pulse quality in κ_{DBR}=200/cm laser was strongly degraded, and κ_{DBR}=40/cm laser has shown no ML pulsations at all.

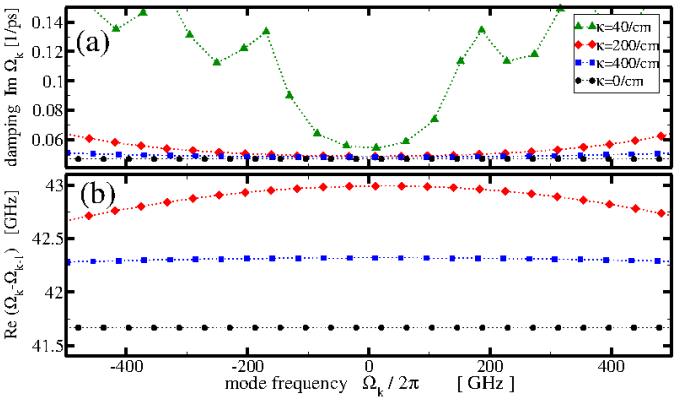

Fig. 4. Calculated mode damping (top) and frequency separation of the adjacent modes (bottom) vs. mode frequency for the FP laser with non-vanishing R_L (black bullets, κ=0) and the lasers with different integrated DBR sections satisfying the relation $\kappa_{DBR} l_{DBR}$=1 and vanishing reflectivity R_L at the DBR section facet.

Our theoretical mode analysis presented in Fig. 4 provides an explanation of experimental observations. An integration of the DBR section introduces a significant modal gain dispersion, supporting only those modes that are within the stop-band of DBR. Consequently, the remaining 4-5 main modes in the laser with κ_{DBR}=40/cm are simply not enough for the formation of the ML pulsations (see green triangles in Fig. 4(a)). On the other hand, the integration of DBRs degrades the equidistance of the modes, which is also a crucial condition for the formation of the ML pulsations (lower panel of the same figure). For the lasers with κ_{DBR}=400/cm this violation is marginal (blue squares in Fig. 4(b)). On contrary, in the lasers with κ_{DBR}=200/cm it becomes important (red diamonds in the same figure) and implies a significant broadening of the RF spectral line.

III. Asymptotic Analysis of the DDE Model

Another model of passive and hybrid ML in lasers with the SA is based on the system of DDEs that is derived from the TW equations under the assumption of a one-directional propagation of the optical fields in the ring cavity (see Ref [8] and Fig. 1(d)):

$$\begin{aligned} \tfrac{1}{\gamma}\tfrac{d}{dt}E + E &= \sqrt{\alpha}\, e^{\frac{(1-i\alpha_g)G(t-T)-(1-i\alpha_q)Q(t-T)}{2}} E(t-T), \\ \tfrac{d}{dt}G &= g_0 - \gamma_g G - e^{-Q}\left(e^{G}-1\right)|E|^2, \\ \tfrac{d}{dt}Q &= \gamma_q\left(1+aF(t)\right)\left(q_0-Q\right) - s\left(1-e^{-Q}\right)|E|^2. \end{aligned} \qquad (4)$$

Here, functions E, G and Q denote the complex field amplitude, the lumped saturable gain and saturable absorber, respectively. The parameters T, g_0, q_0, s, γ, α, $\gamma_{g,q}$, and $\alpha_{g,q}$ represent the field round-trip time in the cold cavity, the pump current in the gain section, the unsaturated absorption in the SA, the ratio of the gain and the SA saturation intensities, the width of the spectral filtering, the linear non-resonant attenuation factor per cavity round-trip including field reflectivity at the facets, the gain and the SA relaxation rates, and the linewidth enhancement factors, respectively. The function $aF(t)$ in this example represents a $1/f_m$-periodic modulation of the negative voltage in the SA, whereas a is the amplitude of this modulation [5]. Such periodic forcing helps to improve the quality of passive ML pulsations. Namely, once the detuning $\delta f = f_p - f_m$ between the passive ML frequency f_p and the modulation frequency f_m is small enough, the pulsation frequency can be entrained by the modulation frequency. These hybrid ML pulsations usually have a reduced time jitter, which is mainly determined by the low jitter of the external modulation.

The experimental and numerical estimation of the frequency detuning ranges admitting hybrid ML for all modulation amplitudes is an important, but also a time-consuming task. In theory, it is related with simulation of many long transient intervals (each one with a slightly modified f_m and/or amplitude a) and a consequent check of the periodicity of the resulting trajectory. The estimation of the hybrid ML existence region in modulation amplitude - detuning plane for a single set of model parameters can take a whole day of

simulations. To accelerate this study, we have investigated the linearization of the DDE model (5) around the passive ML solution in the limit of small modulation amplitude a [5]. We have found a semi-analytic expression for the range of the scaled detuning $\delta f/a$ admitting the existence of the periodic hybrid ML solution. This new technique allows to get reasonable locking range estimates in a couple of minutes so that a more detailed study of the hybrid ML dependencies on all other parameters also becomes possible.

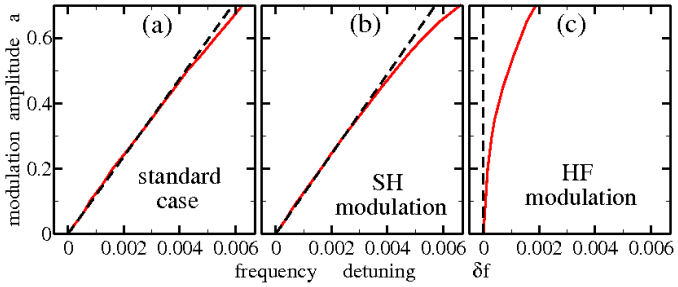

Fig. 5. Estimated length of the interval of the frequency detuning δf admitting periodic hybrid ML state for different modulation amplitudes a for (a): standard, (b): SH, and (c): HF modulations. Thick solid curves: obtained by direct numerical integration of Eqs. (1)-(4) with tuned f_m and a. Thin dashed lines: semi-analytic asymptotic estimates.

The width of the locking range for a selected passively ML state and modulation function $F(t)=\cos(2\pi f_m t)$ is shown in Fig. 5(a). Panels (b) and (c) of the same figure represent the width of the locking regions for the modulation frequency $f_m \approx 2 f_p$ (second harmonic, or SH modulation with $\delta f = f_p - f_m/2$) and $f_m \approx f_p/2$ (half frequency, or HF modulation with $\delta f = f_p - 2 f_m$). The frequency detuning in these cases indicates the difference between f_p and the pulse repetition rate of the hybrid ML (which, in general, differs from the exact frequency of the solution). We note that our algorithms are working properly for standard and SH modulations (solid curves and dashed lines almost coincide), but fail to show a proper locking regions for HF modulation, where the locking range dependence on the amplitude a is nonlinear.

ACKNOWLEDGMENT

This work has been supported by the EU FP7 ITN PROPHET, Grant No. 264687.

REFERENCES

[1] U. Bandelow, M. Radziunas, A. Vladimirov, B. Hüttl, and R. Kaiser, "Harmonic mode-locking in monolithic semiconductor lasers: Theory, simulations and experiment". Optical and Quantum Electronics **38**, 495-512, (2006**)**.

[2] B. Hüttl, R. Kaiser, Ch. Kindel, S. Fiddora, W. Rehbein, H. Stolpe, G. Sahin, U. Bandelow, M. Radziunas, A. Vladimirov, and H. Heidrich. "Experimental investigations on the suppression of Q-switching in monolithic 40 GHz mode-locked semiconductor lasers". Appl. Phys. Lett. **88**, 221104 (2006)

[3] M. Radziunas, A.G. Vladimirov, E.A. Viktorov, G. Fiol, H. Schmeckebier, and D. Bimberg. "Pulse broadening in quantum-dot mode-locked semiconductor lasers: simulation, analysis and experiments". IEEE J. of Quantum Electronics **47**(7), 935 (2011)

[4] M. Radziunas, A.G. Vladimirov, E.A. Viktorov, G. Fiol, H. Schmeckebier, and D. Bimberg. "Strong pulse asymmetry in quantum-dot mode-locked semiconductor lasers". Appl. Phys. Lett. **98**, 031104 (2011)

[5] R. Arkhipov, A. Pimenov, M. Radziunas, D. Rachinskii, A.G. Vladimirov, D. Arsenijevic, H. Schmeckebier, and D. Bimberg. "Hybrid mode locking in semiconductor lasers: simulations, analysis and experiments". IEEE J. of Selected Topics in Quantum Electronics **19**(4), 1100208 (2013)

[6] S. Joshi, C. Calo, N. Chimot, M. Radziunas, R. Arkhipov, S. Barbet, A. Accard, A. Ramdane, and F. Lelarge. "Quantum dash based single section mode locked lasers for photonic integrated circuits". Optics Express **22**(9), 11254 (2014)

[7] U. Bandelow, M. Radziunas, J. Sieber, and M. Wolfrum. "Impact of gain dispersion on the spatio-temporal dynamics of multisection lasers". IEEE J. Quantum Electron., vol. **37**(2), 183 (2001)

[8] A.G. Vladimirov and D. Turaev. "Model for passive mode-locking in semiconductor lasers". Phys. Rev. A **72**(3), 033808 (2005)

[9] M. Radziunas and H.-J. Wünsche. "Multisection lasers: longitudinal modes and their dynamics". Ch. 5 in Optoelectronic Devices - Advanced Simulation and Analysis, ed. J. Piprek, Springer Verlag, New York, (2005)